The Self-interaction of Native TDP-43 C-terminus Inhibits Its Degradation and Contributes to Early Proteinopathies

I-Fan Wang[1,2,*], Hsiang-Yu Chang[1,2,3], Shin-Chen Hou[3], Gunn-Guang Liou[4], Tzong-Der Way[3], C-K James Shen[1]

[1]Institute of Molecular Biology, Academia Sinica, Taipei, Taiwan 115
[2]Garage Brain Science, Taichung, Taiwan 413
[3]Department of Biological Science and Technology, College of Life Sciences, China Medical University, Taichung, Taiwan 404
[4]Division of Molecular and Genomic Medicine, National Health Research Institutes, Miaoli, Taiwan 350

***Corresponding Author**: I-Fan Wang

Author Contributions: I.-F. Wang conceived the research, designed and performed the experiments, wrote the manuscript and coordinated collaboration. H.-Y. Chang performed bioinformatic analysis, conducted the experiments and the data analysis and assisted in writing the manuscript. S.-C. Hou and T.-D. Way assisted in EGCG related experiments and provided reagents. G.-G. Liou carried out the EM. C.-K. James Shen helped in revision of the manuscript.

Key words: TDP-43 C-terminus, Pathological degradation, Frontotemporal lobar degeneration with ubiquitin-positive inclusions (FTLD-U) and amyotrophic lateral sclerosis (ALS), Aggregation-prone domain, Epigallocatechin gallate (EGCG)

ABSTRACT

The degraded, misfolded C-terminus of TDP-43 is associated with a wide spectrum of neurodegenerative diseases, particularly frontotemporal lobar degeneration with ubiquitin-positive inclusions and amyotrophic lateral sclerosis. Cleavage of TDP-43, rather than its phosphorylation or ubiquitination, is the central event of early pathogenesis. However, the precise mechanism of pathological cleavage of TDP-43 remains unknown. We found a novel type of protein-interaction in which native TDP-43 C-terminus protein physically interacts with itself or with cellular-folded yeast prion domain of Sup35 forming dynamic aggregates. This prion-like nature governs known cellular functions of TDP-43, including subcellular localization and exon skipping of CFTR. Significantly, mutants with a failure to engage in prion-like interactions were cleaved into a ~24 kDa C-terminus fragment of TDP-43. The estimated cleavage site of the degraded TDP-43 fragment corresponds to the pathological-cleavage site identified in patients with TDP-43 proteinopathies. Consistently, constraining the prion-like interactions of these mutants using EGCG attuned pathological-like degradation. Briefly, the native function of the TDP-43 C-terminus acts as a guardian of pathogenesis, which is directly associated with loss of function. Moreover, our insights into native aggregation-prone domains further explain the reciprocal effects of TDP-43 proteinopathies and other misfolding diseases in their early stage of pathogenesis.

INTRODUCTION

The aggregation of misfolded, phosphorylated, ubiquitnated C-terminal fragments of TAR DNA-binding protein 43 (TDP-43) is a common characteristic in frontotemporal lobar degeneration with ubiquitin-positive inclusions (FTLD-U) and amyotrophic lateral sclerosis (ALS)[1-8]. Among mammals, zebrafish and flies, the protein sequence, biochemical properties and biological functions of TDP-43 are well conserved. In the cell nucleus, TDP-43 forms visible 50- to 250-nm granules that serve as a scaffold to link other functionally related sub-compartments and participates in transcriptional repression as well as alternative splicing[9-12]. TDP-43 specifically binds to UG repeat sequences in RNA, altering pre-mRNA splicing of cystic fibrosis transmembrane conductance regulator (CFTR) and may associate with long ncRNA to regulate nuclear speckle or paraspeckle[11, 13]. TDP-43 mutants lacking a C-terminal glycine-rich region fail to excise exon 9 in the CFTR gene[9], but how TDP-43 C-terminus governs exon 9 skipping of CFTR, as well as its role in pathogenesis of TDP-43 proteinopathies is still unknown. Given that the TDP-43 C-terminus binds directly to hnRNP A1 and hnRNP A2/B1 in pull-down assays[14], the loss of association between TDP-43 and the hnRNPs has been proposed as a possible mechanism behind TDP-43 proteinopathies, causing aberrant

pre-mRNA splicing or mislocalization of TDP-43. However, this hypothesis does not adequately account for pathological degradation of TDP-43 protein itself, which is a major feature of TDP-43 proteinopathies in the early stage[1].

Recently, we have reported a database search for homologs of the mTDP-43 C-terminus across multiple species and found that the mTDP-43 C-terminal domain (a.a. 274-414) shares 24.2% sequence identity with the N-terminal yeast prion domain of Sup35 (a.a. 1-125; SupN)[15]. This analysis led us to propose that the TDP-43 C-terminus might have prion-related properties. Based on the atypical Q/N rich-domain of TDP-43 involved in the self-assembly of misfolded C-terminal fragments and the sequestration of TDP-43 into polyglutamine aggregates, TDP-43 has been further proposed to act as a prion[16]. However, in contrast to most known prions, misfolded pathological fragments of TDP-43 or full-length TDP-43 aggregates *in vitro* do not react with the amyloid-specific dye Congo Red[1,17], indicating that the TDP-43 Q/N-rich domain may not be a prionogenic domain. We were, thus, interested in understanding whether the intriguing sequence similarity in Q/N residues between the TDP-43 C-terminus and known prion domains is critical to the cellular functions of TDP-43 C-terminus, rather than misfolded related. However, to date, no cellular roles have been clearly elucidated for a prion

domain. To gain insight into its cellular role, we developed assays to explore the native functions of TDP-43 C-terminus in cells.

RESULTS

Highly Dynamic Assembly of TDP-43 Aggregates in Normal Cells via Q/N-rich C-terminus

Based on structure and intensity, two groups of TDP-43 clusters appeared in the nucleus: visible granules of 50-250 nm in diameter (arrow, Fig. 1a) and irregular puncta (arrowhead, Fig. 1a), as shown by endogenous TDP-43 and GFP-tagged, full-length mTDP-43 (TDP-43-FL) (Fig. 1a). The dynamics of TDP-43 clusters in living cells were further visualized by time-lapse microscopy. In GFP-TDP-43-FL transfected cells, the small irregular puncta were rapidly burst, reorganized, or disassembled, and were restricted to a local area (Fig. 1b). High magnifications of irregular puncta of GFP-TDP-43-FL are shown in Fig. 1b (arrowheads, lower panel). Individual GFP-TDP-43 small puncta histories suggest that they have similar motility characteristics. In contrast, most of the visual granules were more stable and traveled within a limited localization. A few granules were stationary (white arrowheads, Fig. 1c). Also observed, but rare, were fission and fusion events (yellow arrowheads and red arrowheads,

respectively, Fig. 1c). Occasionally two independent granules of GFP-TDP-43-FL from two different areas collided and then separated (blue arrowheads), possibly exchanging material between granules (Fig. 1c). With gentle 0.5% Triton X-100 pre-extraction of cells to remove diffuse nucleoplasmic TDP-43 proteins, TDP-43 clusters in nuclei exhibit clear shapes by immunostaining (Fig. 1d, middle)[18]. An example of a nucleus is shown in Fig. 1d. No signal was detected in cells without permeabilization (Fig. 1d, right). Western blot further confirmed that a fraction of mTDP-43 FL proteins was retained in the detergent-insoluble fraction (Fig. 1e, left lane). These results suggest that these insoluble supermolecules of TDP-43 protein, behave as highly dynamic functional aggregates in the nucleus.

An atypical Q/N-rich domain of TDP-43 is capable of spontaneously forming a filamentous structure and retains TDP-43 proteins in the insoluble fraction in mammalian cells in the same way as other aggregation-prone domains (Supplementary S1). To validate whether the aggregation propensity of TDP-43 C-terminus contribute to form functional TDP-43 aggregates in physiology statues as well, we constructed a TDP-43 C-terminal deletion mutant, TDP-43-PLDΔ. In the absence of the PLD, TDP-43-PLDΔ diffused in the nucleus (Fig. 1f). We termed the region as prion-like domain (PLD)[19]. It

appears that, in addition to forming misfolding aggregates, the Q/N-rich domain is essential for the assembly of reversal functional TDP-43 aggregates in cells.

Functional Substitutions of GQN-rich C-terminus of Mammalian TDP-43 by a Yeast Prion Domain of Sup35

To clarify the intriguing sequence similarity in Q/N residues between the TDP-43 C-terminus and yeast prion domain of Sup35 (SupN), we replaced the PLD of GFP-tagged mTDP-43 with yeast prion domains (TDPSupN) (Fig. 2a). As the sequence homology or the polyQ/N context may affect the conformation in cells, an additional replacement by the N-rich yeast prion domain, UreN (aa. 1-84) was also generated. UreN shares only 12% similarity with the PLD. The distribution of the Q and N residues of these three Q/N-rich domains was illustrated in Fig. 2b. Interestingly, chimeric TDPSupN proteins restored two groups of clustering aggregates: visible granules of 50-250 nm in diameter (arrow, Fig. 2c) and irregular puncta (arrowhead, Fig. 2c) in the nuclei, as shown by the GFP-tagged, full-length mTDP-43 (mTDP-43-FL). In contrast, mTDPUreN failed to recapitulate full-length TDP-43 localization, although mTDPUreN formed large foci in the cytosol (Fig. 2c). Live-cell imaging showed that the clustered mTDPSupN

proteins had identical behavior to mTDP-43-FL. Fluorescence recovery after photobleaching (FRAP) analysis of GFP-mTDP-43-FL and GFP-mTDPSupN movement showed that fluorescence recovery of these proteins was rapid, but significantly slower than that of mTDP-43-PLDΔ (Fig. 2d). The half-recovery time was calculated to be 8.23s, 7.28s and 1.34s, for GFP-mTDP-43-FL, GFP-mTDPSupN, and GFP-mTDP-43-PLDΔ, respectively. The recording images obtained from two bleached areas of a single GFP-mTDPSupN expressing cell showed fluorescence recovery (Fig. 2e). We noticed that the fluorescence recovery in visible granules was faster than that in irregular puncta, which may imply differential kinetics in the redistribution of protein into the two types of functional aggregates (Movie 1). Significantly, *in vivo* splicing assays revealed that mTDPSupN effectively promoted exon 9 skipping of CFTR in the same way as TDP-43-FL (Fig. 2f and Supplementary S2). Cotransfection with α-globin promoter and mTDPSupN in 293T cells did not alter mTDP-43 transcription repression (Supplementary S3). As expected, the C-terminus of TDP-43 was not involved in TDP-mediated transcriptional repression[12]. In summary, mTDPSupN localized to the nucleus, where it effectively promoted exon 9 skipping in the same manner as endogenous TDP-43.

As GFP-TDP-43-FL and GFP-TDPSupN proteins dynamically clustered in the nucleus, we examined whether self-interaction of TDP-43 occur via prion-like domain. Using co-immunoprecipitation with FLAG antibodies, we found that endogenous 43-kD and 95-kD TDP proteins co-precipitated with FLAG-tagged TDP-43, suggesting TDP-43 self-interaction (Fig. 2g). 95-kD TDP-43 protein was likely constituted by a 43-kD TDP-43 and a 52-kD ubiquitinated TDP-43 (Supplementary S4). This self-interaction can be recapitulated by GFP-tagged FL and mTDPSupN (Fig. 2h). Notably, the coprecipitation efficiency of endogenous TDP-43 with mTDPSupN was similar to that with TDP-43 FL, and more effective than with TDP-43-PLDΔ (Fig. 2h). These results suggested that the cellular role of the Q/N-rich domain is to promote protein self- or cross-interactions and act as a protein-protein interaction domain in the cell.

Comparisons among the cellular and misfolded properties of the known Q/N-rich domain were shown in Table 1[20-31]. The cellular-folded Q/N-rich domain shared key properties characteristic of the misfolded proteins, including insolubility and a tendency to form aggregates via intrinsic element- and self-interactions. However, the interaction of these prion-like supramolecules was dynamic in the cell in response to stimuli. We hypothesized that these interactions occur because of the structural plasticity of the

aggregation-prone domain, which allows temporal folding of parallel β-sheets in the cell. We thus described this interaction of cellular-folded Q/N-rich domain as "prion-like interaction". Notably, although natively folded Sup35N and natively folded TDP-43 C-terminus adopt substitutable structure in cells, only Sup35N aggregate into an in-register β-sheet amyloid structure when misfolded, suggesting that a protein that has prion-like properties does not have to be a prion.

A Single Proline Substitution at Aggregation-prone-domain of TDP-43 Induced Pathological Degradation of TDP-43

Substitution of the structural breaking amino acid proline has been demonstrated to destroy β-sheets[32]. The simplified model was illustrated in Fig. 3a. As glycine- rich region localizes at adjacent the 1st Q/N rich region, two glycine residues G296 and G300 were selected to examine the effect of glycine on prion like nature of TDP-43 C-terminus. We thus substituted proline at amino acids G296, G300, Q302 or Q340 of TDP-43 PLD (Fig. 3b). Notably, only TDP-43 Q302P proteins were partially degraded into ~24kD pathological fragments (asterisk, Fig. 3b). *In vivo* splicing assay showed that TDP-43 Q302P attenuated exon 9 skipping efficiency by 23.5% (Supplementary S5). Four days post-transfection with Q302P, a portion of the transfected cells showed cytoplasmic accumulation of TDP-43 Q302P fusion proteins (arrow, Fig. 3c) and formed cytosolic

aggregates (arrowhead, Fig. 3c). The ratio of cells with cytoplasmic accumulated fusion proteins in TDP-43-FL and TDP-43 Q302P- expressing transfectants was shown in Fig. 3d. Indeed, a subset of the TDP-43 Q302P-expressing cells had a lower fluorescence half-recovery time, which was similar to that of TDP-43-PLDΔ (Fig. 3e). A lower viability of TDP-43 Q302P-expressing cells was further confirmed by MTT assay (Supplementary S6).

Furthermore, substitution of proline at amino acid 25 of Sup35 has been suggested to abolish the propagation and infectivity of all three [PSI] variants[33]. To confirm that impairing the cellular properties of "prion domain" leads to pathological degradation of TDP-43 proteins, we generated a mTDPSupN mutant, GFP-mTDPSupN*, which contained a G25P substitution in SupN, and assessed its localization and ability to skip exon 9 of CFTR. As expected, immunoblot analysis showed that the majority of GFP-mTDPSupN* proteins shifted to the soluble fraction and were degraded into ~48-kD fragments (Fig. 3f). The estimated cleavage site of the degraded mTDPSupN* fragment corresponded to the cleavage site of a ~24 kD fragment that has been detected in patients with TDP-43 proteinopathies[1]. Tubulin and actin immunoblot were used as controls for non-specific protein degradation (lower panel, Fig. 3f). The degraded mTDPSupN* fragment did not translocate into the insoluble fraction, possibly because a

G25P substitution in SupN* completely abolished the intrinsic propensity of mTDPSupN* to aggregate. GFP-mTDPSupN* was evenly distributed in the nucleus and cytosol (Fig. 3g) and failed to promote alternative splicing activity that confirmed loss of functional prion-like domain of TDP-43 (Fig. 3h).

Epigallocatechin Gallate (EGCG) Induced Oligomerization of TDP-43 that Attuned Its Protein Degradation

If the disruption of prion-like interactions of the Sup35 or TDP-43 C-terminus leads to a shift into the soluble fraction and protein degradation (Fig. 3), constraining prion-like domains should cause oligomerlization/functional aggregates and then impede the cleavage of TDP-43 proteins. EGCG has been suggested to redirect an array of amyloidogenic molecules, including synuclin, huntingtin, amyloid-β, TTR and yeast prion [PSI], into nontoxic oligomers. A recent study of crystallization of a V30M TTR-EGCG complex further indicated that EGCG directly bound and stabilized TTR tetramer in vitro and induced TTR oligomerization in cells[34]. The pharmaceutical mechanism of EGCG curing of yeast prions [PSI] could be via stabilization of the native prion domain Sup35 as well[35]. To address this, EGCG was applied to block the rapidly

degraded mutant proteins of TDPSupN* proteins (Fig. 4a). TDPSupN* mutants were treated with mock or 20 μM EGCG. An increase in full-length TDPSupN* in cells treated with 20 μM EGCG for 3 days relative to the level in mock-treated cells was observed (Fig. 4a). We further speculated that EGCG may function in preservation of the native folded TDP-43 C-terminus as well (Fig. 2c, f, h). Indeed, EGCG induced oligomerization of TDP-43 in a dosage-dependent manner (Fig. 4b). In GFP-Q302P-TDP-43 expressing cells with rapid degradation, the degradation of GFP-Q302P-TDP-43 proteins was reduced by EGCG and corresponded with the appearance of TDP-43 aggregates in nuclei (Fig. 4c and d). To confirm that EGCG-induced aggregation was mediated via TDP-43 C-terminus, GFP-TDP-43-FL or GFP-TDP-43-PLDΔ expressing cells were treated with 20 μM EGCG. Upon stimulation of EGCG, GFP-TDP-43-FL proteins aggregated in nuclei (arrow), but GFP-TDP-43-PLDΔ proteins did not (Fig. 4e). MTT assay further confirmed that these EGCG-induced TDP-43 aggregates were non-toxic (Fig 4f). In confluence-cultured cells, with EGCG 20 or 50 μM, the normal protein degradation of GFP-TDP-43-FL expressing cells also attuned (Fig. 4g left). Consistent with the increase of TDP-43 aggregates upon EGCG, the insoluble protein level of GFP-TDP-43-FL increased simultaneously (Fig. 4g right). The identical effect of EGCG on endogenous TDP-43 proteins was observed in confluence-cultured cells (Supplementary S7). Taken

together with the results of Figure 3, we concluded that the impairment of interactions between the cellular-folded prion domains is a prerequisite for its protein degradation under both normal and pathological conditions.

DISCUSSION

Increasing evidence indicates that aggregation-prone domains play crucial roles in various cellular functions, such as granular assembly and nuclear export (Table 1). In this study we further found that the Q/N-driving propensity of TDP-43 is involved in alternative splicing and protein stability. Recently an increasing number of prionogenic domain-containing proteins have been identified, among them many, such as Mot3p and Lsm4p, contain a Q/N-rich domain and are involved in transcription or RNA processing[36]. Additionally, a self-perpetuating Q/N-rich domain of apCPEB was suggested to participate in the long-term facilitation of Aplysia[31]. A set of proteins which control the stability of mRNAs as well as their translational silencing are co-localized in cytoplasmic foci called processing bodies or P bodies[37]. Interestingly, several P-body components contain a potential prionogenic domain. In yeast, the prion-like properties of this motif may be related to granule assembly and can be restored by replacement with yeast prion RNQ1. Lsm4p is one of these well characterized proteins[27]. Ultrastructural studies have

demonstrated that P-bodies are condensed, fibrillar aggregates as that of the prion [PSI] particles in yeast[38,39]. In the same way as shown here in the assembly of TDP-43 functional aggregates, assembly of P-bodies is dynamic and, in neurons, is regulated by neuronal activity[41]. In consistent with this kind of physiological aggregates, a new type of off-pathologenesis pathway contains a non-toxicity ~ 500 kD oligomer of amyloidogenic molecules has been found in cells[42]. We suggested that the higher bands of TDP-43 shown in Fig. 2h-g, would be assembled prion-like oligomers of TDP-43, as the overexpressing TDP-43 Q302P interfered the generation of endogenous higher bands of TDP-43 upon oxidative stress (Unpublished data).

Based on the results of the current study we propose a model, outlined in Fig. 5, in which the ambivalent propensity of the TDP-43 C-terminus allows to either form structurally flexible aggregates under physiological processes (Fig. 5, conformer B and conformer B'), or rigid pathological inclusions (Fig. 5, conformer C). The restorative formation of nuclear clustering and alternative splicing ability when TDP-43 C-terminus is replaced by yeast sup35N strongly suggests that a prion-like property is involved in subcellular localization and exon 9 skipping of CFTR (Fig. 4). Interestingly, ALS-inherited G348C and R361S mutants attenuated exon 9 skipping efficiency by

12.5% and 28.9%, respectively, whereas G296P, a disease-unrelated mutant, did not (Supplementary S8). These results implied that ALS-inherited mutations showed attenuation of the prion-like activity of TDP-43. We prefer that the impairment of interactions between prion-like domains occurs prior to caspase cleavage, since an oligomer stabilizer, EGCG can reduce protein degradation of TDP-43 mutants defected in prion-like interaction (Fig. 4a, c, d). The failure of the PLD to adopt proper cellular folding, due to a loss of prion-like interactions or impairment by ALS-linked mutations at the early stages of pathogenesis, may trigger pathological fragment cleavage, convert the PLD to a misfolded structure, and ultimately result in disease inclusions. We also found that the TDP-43 N-terminus stabilized the cellular-folded conformation and altered the insoluble propensity of TDP-43 C-terminus, suggesting that the TDP-43 N-terminus (1-105) may act as a chaperon-like domain to autoinhibit the disorder tendency of the PLD through long-range intramolecular interaction (Supplementary S9). A recent study showed that physical interaction of mutant SOD1 proteins with the TDP-43 N-terminus consistently resulted in an increase in TDP-43 proteins in the detergent-insoluble fraction[43]. The comparison of TDP-43 variants is summarized in table S1.

Additionally, the co-immunoprecipitation of endogenous TDP with mTDPSupN

suggested that prion-like properties mediate the interactions between heterogenous Q/N-rich domains (Fig. 2). Indeed, we have found that proteins containing polyQ domains are often functionally linked to other poly-(amino acid) proteins by database analysis (http://string.embl.de/newstring_cgi/) of the functional interactomes of Q/N-rich proteins. For example, functional interactome analysis of ATXN2 reveals ten functional interactors. Seven of the ten interactors, FOX1, TBP, ATN1, CACNA1A, ATXN1, ATXN3, ATXN7 and DDX6 contain a polyQ-rich element. In addition to the mTDPSupN used in this study, TDP-43 has recently been shown to interact with DDX6 and ATXN2[44,45,46]. These three Q/N-rich proteins could physically interact each other and localize to stress granules or P-bodies under certain conditions[45]. More recently, Elden *et al.* demonstrated that treatment with RNase abolished co-immunoprecipitatation of ATXN2 with TDP-43-YFP, suggesting that the interaction of ATXN2 and TDP-43 occurs in an RNA dependent manner[44]. With regard to the RNA dependent regulation of TDP-43 activity, we found that RNA binding deficient mutants of TDP-43 proteins would form visible granular aggregates and gained a ~20-fold TDP-43 visiable granules in nucleus (Supplementary S10a)[44]. The relocalization of TDP-43 proteins from irregular puncta to visible granules, where TDP-43 did not bind to RNAs, suggests that prion-like activity may be regulated by RNA binding then affecting TDP-43 functions. We propose that the

Q/N-rich element of TDP-43 can be exposed when RNAs bind to TDP-43. The allosterism can allow natively folded TDP-43 to interact with natively folded ATXN2 or DDX6 in a prion-like manner (Fig. 5, conformer B). In the presence of RNAse, a significant shifting of TDP-43 from monomer to dimer was observed by western blotting analysis (Supplementary S10b). This result was consistent to observations in supplementary S9a and c, and supported in absent of RNA, TDP-43 proteins formed the other type of functional aggregates, proposed as conformer B' of Fig. 5.

The cross- interactions between "cellular folded Q/N-rich domains" provide an explanation for the reciprocal effects of prone-to-aggregation protein in common protein misfolding disease. The biochemical and biophysical roles of the cellular folded Q/N-rich domain are likely to retain the protein in the insoluble fraction by self- or cross-interaction (Fig. 2 and Table 1). This function would allow the protein to form dynamic scaffolds in a stable conformation and have a lower mobility, which is suited for restricting the protein to a microenvironment optimal for performing particular bio-reactions, such as alternative splicing and sub-compartment assembly.

As the aggregation-prone domain has structural plasticity and can spontaneously

self-assemble into ordered pathological or functional aggregates, it is reasonable to speculate that these two pathways may act antagonistically, as shown in Fig. 5. Ideally, compounds that stabilize functional aggregates of aggregation-prone domains may be investigated as therapies for protein misfolding. This is particularly important for TDP-43 proteinopathies, because cleavage of TDP-43 proteins occurs prior to inclusion formation during disease progression. Loss of normal full-length TDP-43 proteins perturbs pre-mRNA splicing and ultimately leads to cell death. Growing evidence shows that polyphenol compounds, such as EGCG, redirect an array of amyloidogenic molecules and effectively cured huntingtin inclusions by oral administration in a *Drosophlia melanogaster* model[47,48]. In our studies, EGCG induced oligomerlization of natively folded TDP-43 and thus inhibited pathological-like degradation, suggested targeting to stabilization of natively folded prion domains is a promise therapeutic approach for FTLD-U and ALS. With an eye to therapy design for command of cellular- folded aggregation- prone domain, future work should focus on the resolution of an accurate cellular structure of the TDP-43 C-terminus and the identification of factors affecting prion-like interactions under physiological and pathological processes. A potential mechanism could be the interplay of post-translation modifications on the prion-like domain.

References and Notes

1. M. Neumann *et al*. *Science* **314,** 130 (2006).

2. M. Neumann, L. K. Kwong, D. M. Sampathu, J. Q. Trojanowski, V. M. Lee. *Arch. Neurol.* **64,** 1388 (2007).

3. E. Kabashi *et al*. *Nat. Genet*. **40,** 572 (2008).

4. M. J. Winton *et al*. *J. Biol. Chem.* **283,** 13302 (2008).

5. W. L. Lin, D. W. Dickson. *Acta Neuropathol.* **116,** 205 (2008).

6. M. Hasegawa *et al*. *Ann. Neurol.* **264,** 60 (2008).

7. I. F. Wang, L. S. Wu, H. Y. Change, C. K. Shen. *J. Neurochem.* **105,** 797 (2008).

8. Y. J. Zhang *et al*. *Proc. Natl. Acad. Sci. U.S.A.* **106,** 7607 (2009).

9. H. Y. Wang, I. F. Wang, J. Bose, C. K. Shen. *Genomics*. **83,** 130 (2004).

10. S. H. Ou, F. Wu, D. Harrich, L. F. Garcia-Martinez, R. B. Gaynor. *J. Virol.* **69,** 3584 (1995).

11. E. Buratti *et al*. *EMBO J.* **20,** 1774 (2001).

12. I. F. Wang, N. M. Reddy, C. K. Shen. *Proc. Natl Acad. Sci. U.S.A* **99,** 13583 (2002).

13. J. R.Tollervey *et al. Nat Neurosci* **14**, 452 (2011).

14. E. Buratti *et al*. *J. Biol. Chem.* **280,** 37572 (2005).

15. I. F. Wang, L. S. Wu, C. K. Shen. *Trends Mol. Med.* **14,** 479 (2008).

16. R. A. Fuentealba *et al*. *J. Biol. Chem.* **285,** 26304 (2010).

17. B. S. Johnson *et al*. *J. Biol. Chem.* **284,** 20329 (2009).

18. D. B. Bregman, L., Du, S. van der Zee, S. L. Warren. *J. Cell Biol.* **129,** 287 (1995).

19. B. S. Johnson, J. M. McCaffery, S. Lindquist, A. D. Gitler. *Proc. Natl. Acad. Sci. U.S.A.* **105,** 6439 (2008).

20. S. Brandner *et al*. *Nature* **379,** 339 (1996).

21. S. V. Paushkin, V. V. Kushnirov, V. N. Smirnov, M. D. Ter-Avanesyan. *EMBO J.* **15,** 3127 (1996).

22. M. M. Patino, J. J. Liu, J. R. Glover, S. Lindquist. *Science* **273,** 622 (1996).

23. H. L. True, S. L. Lindquist. *Nature* **407,** 477 (2000).

24. I. L. Derkatch *et al*. *Proc. Natl. Acad. Sci. U.S.A.* **101,** 12934 (2004).

25. N. Gilks *et al*. *Mol. Biol. Cell* **15,** 5383 (2004).

26. M. Tanaka, P. Chien, N. Naber, R. Cooke, J. S.Weissman. *Nature* **428,** 323 (2004).

27. C. J. Decker, D. Teixeira, R. Parker. *J. Cell Biol.* **179,** 437 (2007).

28. Y. A. Vitrenko, E. O. Gracheva, J. E. Richmond, S. W. Liebman. *J. Biol. Chem.* **282,** 1779 (2007).

29. R. B. Wickner, F. Shewmaker, D. Kryndushkin, H. K. Edskes. *Bioessays*. **30,** 955 (2008).

30. C. Ader *et al. Proc. Natl. Acad. Sci. U.S.A.* **107,** 6281 (2010).

31. K. Si, Y. B. Choi, E. White-Grindley, A. Majumdar, E. R. Kandel. *Cell* **140,** 421 (2010).

32. C. Soto, M. S. Kindy, M. Baumann, B. Frangione. *Biochem Biophys Res Commun.*

226, 672 (1996).

33. H. Y. Chang, J. Y. Lin, H. C. Lee, H. L. Wang, C. Y. King. *Proc. Natl. Acad. Sci. U.S.A.* **105,** 13345 (2008).

34. M. Miyata *et al. Biochemistry* **49**, 6104 (2010).

35. B. E. Roberts *et al. Nat Chem Biol.* **5**, 936 (2009).

36. S. Alberti, R. Halfmann, O. King, A. Kapila, S. A. Lindquist. *Cell* **137,** 146 (2009).

37. M. Fenger-Grøn, C. Fillman, B. Norrild, J. Lykke-Andersen. *Mol. Cell* **20,** 905 (2005).

38. S. Souquere *et al*. *J Cell Sci.* **122,** 3619 (2009).

39. S. Kawai-Noma *et al. J Cell Biol*. **190,** 223 (2010).

40. We are grateful to Dr. C.-H. Wong at Academia Sinica for discussion and proofreading, to Dr. Carmay Lim at Academia Sinica for providing structural insights, to Tsung-Yu Tsai for her assistance in writing this article and to Dr. F. Baralle at the International Centre for Genetic Engineering and Biotechnology in Italy for providing us with the hCF-TG13T5 minigene plasmid. We also thank the staff of the Imaging Core of IMB, Academia Sinica. This research was supported by Academia Sinica, National Health Research Institutes and National Science Council grants to C.-K. James Shen (NSC 99-2321-B-001-033-) and G.-G. Liou (MG-099-PP-08) and Garage Brain Science, Com (ND-01-001). I.-F. Wang

dedicates this article to her late sister.

LEGENDS

Figure 1. Dynamics of Detergent-Insoluble TDP-43 Aggregates in Normal Cells (**a**) GFP-mTDP-43-FL, as endogenous TDP-43, formed dispersed visible granules (arrow) and irregularly shaped puncta (arrowhead) in the cell nucleus. Scale bars: 10 μm. (**b**) Visualization of supramolecular GFP-mTDP-43-FL proteins by time-lapse microscopy. Supramolecular GFP-mTDP-43-FL proteins can be classified into two groups on the basis of their structure and dynamics. Time-lapse fluorescent image of GFP-mTDP-43-FL expressing cells were taken every 1 min for 30 min. Arrowheads in high-magnification images, upper panels, are shown to demonstrate the dynamics of irregularly shaped puncta. Scale bars: 10 μm. (**c**) Tracking of visible granules of GFP-mTDP-43-FL. White arrowheads indicate stationary granules; yellow arrowheads indicate fission; red arrowheads indicate fusion; blue arrowheads indicate the collision and separation of two distinct granules. (**d**) Pre-extraction of nucleoplasmic proteins revealed clear TDP-43 aggregates in 293T cells. In the regular protocol (fixation/permeabilization; F/P), transfectants were fixed with 3.75% paraformadehyde and permeabilized with 0.5% Triton X-100. In the pre-extraction protocol (P/F), transfectants were extracted with 0.5% Triton X-100, and then fixed with 3.75% paraformaldehyde.

Cells without permeabilization (F) were used as a negative immunostaining control. These fixed 293T cells were then immunostained with antibodies against TDP-43. Images of cells were acquired by confocal microscopy. (**e**) Validation of the solubility of GFP- mTDP-43-FL by western blot. The protein lysate harvested from GFP-mTDP-43-FL-expressing 293T cells was used for immunoblotting with anti-GFP antibody. (**f**) The disordered C-terminus of mTDP-43 (prion-like domain; PLD) is required for induced granular assembly. In contrast to full-length TDP-43 (mTDP-43-FL), mTDP-43-PLDΔ appears evenly distributed in nuclei without TDP granules.

Figure 2. Functional Substitutions of the GQN-rich, C-terminus of Mammalian TDP-43 by a Prion Domain SupN. (**a**) Scheme of GFP-tagged chimerical mTDP-yeast prion domain fusion construct. (**b**) Illustration of Q/N distribution in the PLD, yeast prion domain Sup35 (1-125) (SupN) and UreN (1-84). (**c**) Localization of GFP-tagged mTDPSupN and mTDPUreN. Replacement of the PLD with SupN restored nuclear clustering in the manner of GFP-mTDP-43-FL. The construct mTDPSupN formed dispersed visible granules (arrow) and irregularly shaped puncta (arrowhead) in the cell nucleus. mTDPUreN formed

large foci in cytosol. Scale bars: 10 μm. (**d**) Visualization of TDP-43-FL proteins and TDPSupN proteins by time-lapse microscopy. FRAP analysis of GFP-TDP-43-FL, GFP-TDPSupN and GFP-TDP-43-PLDΔ movement. (**e**) Selected images of TDPSupN expressing cells demonstrate fluorescence recovery of GFP-tagged TDP-43 proteins. (**f**) Further examination of the alternative splicing ability of GFP-tagged mTDPSupN by *in vivo* splicing assay. The chimera mTDPSupN promoted exon-9 exclusion in a manner similar to TDP-43-FL. Exon-9 inclusion (+) and exon-9 exclusion (-) bands are indicated. All data are presented as means with SD (n = 3). M: marker; *: aberrant splicing product. (**g**) An examination of TDP-43 self-interaction *in vivo* by cross-IP. The protein lysate harvested from Flag- or Flag-TDP-43-expressing 293T cells was used for immunoprecipitation with anti-Flag antibody and was further examined by immunoblotting with anti-TDP antibody. Endogenous 43 kD TDP and 95 kD TDP were co-precipitated with Flag-TDP-43. (**h**) Co-precipitation efficiency of mTDP-43 variants with 95 kD TDP and 43kD TDP. The co-purification of TDP-43 with associated proteins was performed by cross-IP analysis with anti-GFP antibody from the lysate of overexpressing GFP-tagged mTDP-43 variants FL, PLDΔ, or TDPSupN. The immunoprecipitates were further examined by

immunoblotting with an anti-TDP antibody. SupN complemented PLD in interaction with endogenous TDP.

Figure 3. A proline Substitution in the Prion Domain of mTDPSupN or TDP-43 C-terminus Abolishes the Prion-like Interaction and Induces Pathological Degradation of TDP-43 Proteins. (**a**) As illustrated, Proline substitution could abolish the clustering of PLD if the substitute resides in a b-sheet (top); Proline substitution has no effect on the clustering if the substitute resides in a loop region (bottom). (**b**) Immunoblot analysis of G296P, G300P, Q302P and Q342P mTDP-43 mutants. Linear illustration of the mutations substituted with proline is shown in the upper panel. Anti-GFP antibodies were used for the immunobloting. Note that TDP-43 Q302P substitution resulted in a pathological fragment indicated by an asterisk. (**c**) At 4 days post-transfection, cytosplasmic accumulation (arrow) and aggregation (arrowhead) was significantly increased in the TDP-43 Q302P-expressing cells. Scale bar: 20 μm. (**d**) Statistical analysis of cells with TDP-43 proteins accumulated in the cytosol for TDP-43-FL and TDP-43 Q302P transfectants. (**e**) Comparisons of half-recovery time of fluorescence between GFP-TDP-43-FL proteins, GFP-TDP-43-PLDΔ proteins and

GFP-TDP-43 Q302P proteins by FRAP. In a small portion of TDP-43 Q302P-expressing cells, GFP-TDP-43 Q302P proteins have a lower half-recovery time similar to the GFP-TDP-43-PLDΔ proteins. (**f**) A G25P substitution in the prion domain of mTDPSupN abolishes the prion-like interaction and induces pathological degradation of mTDPSupN proteins. A biochemical analysis of mTDPSupN and mTDPSupN* proteins was examined using anti-GFP antibodies. The construct mTDPSupN*, but not mTDPSupN, was cleaved into a ~48 kD fragment (*) and a 32 kD fragment. Tubulin and actin immunoblots were used as controls for non-specific protein degradation. (**g**) Localization of GFP-tagged mTDPSupN*. In contrast to GFP-tagged mTDPSupN, GFP-tagged mTDPSupN* appeared diffuse in the cytosol and the nucleus of 293T cells. Scale bar: 10 μm. (**h**) Deficiency of CFTR exon-9 skipping by GFP-tagged mTDPSupN*. Exon-9 inclusion (+) and exon-9 exclusion (-) bands are indicated. M: marker; *: aberrant splicing product. All data are presented as means with SD (n = 3).

Figure 4. The Effects of Epigallocatechin Gallate (EGCG) on TDP-43. (**a**) Stimulation with 20 μM EGCG increased the full length of TDPSupN*. The TDPSupN*-expressing cells were treated with or without EGCG for 3 days and

were then harvested for analysis using anti-GFP antibodies. *Full length. All data are presented as means with SD (n = 3). (**b**) EGCG induced oligomerization of TDP-43. A biochemical analysis of endogenous proteins with or without EGCG using anti-TDP-43 antibodies. The quantification of the oligomeric TDP-43 proteins is shown in the right panel. All data are presented as means with SD (n = 3). *P < 0.05 by ANOVA. (**c**) EGCG attuned the protein degradation of GFP-Q302P-TDP-43. (**d**) Upon EGCG addition, GFP-Q302P-TDP-43 aggregates (arrow) appeared by using anti-GFP antibodies. Scale bar: 10 μm. (**e**) Failure of induced PLD truncated mTDP-43 mutant to form aggregates by EGCG. Scale bar: 10 μm. (**f**) MTT assay of viability of TDP-43-FL-expressing cells given EGCG. All data are presented as means with SD (n = 5). (**g**) A biochemical analysis of GFP-TDP-43-FL proteins with or without EGCG using anti-GFP antibodies.

Figure 5. Working Model for the Intrinsic Propensities of TDP-43 C-terminus in Normal Cellular Functions and Disease Progression. As part of the normal physiological processes of the cell, the intrinsic propensity of the TDP-43 C-terminus is to confer assembly of nuclear bodies, protein stability, and promote exon9 skipping of CFTR by adopting flexible prion-like folding; however, if loss of

TDP-43 N-terminus by pathological cleavage, ALS-linked mutations or other unknown cellular factors could cause disruption of cellular prion-like folding of the TDP-43 C-terminus, TDP-43 inclusions will form. EGCG induced oligomerization of TDP-43 and reduced its degradation.

Table 1. Properties of Cellular-folded and Misfolded Q/N-rich Domain.

Figure 1

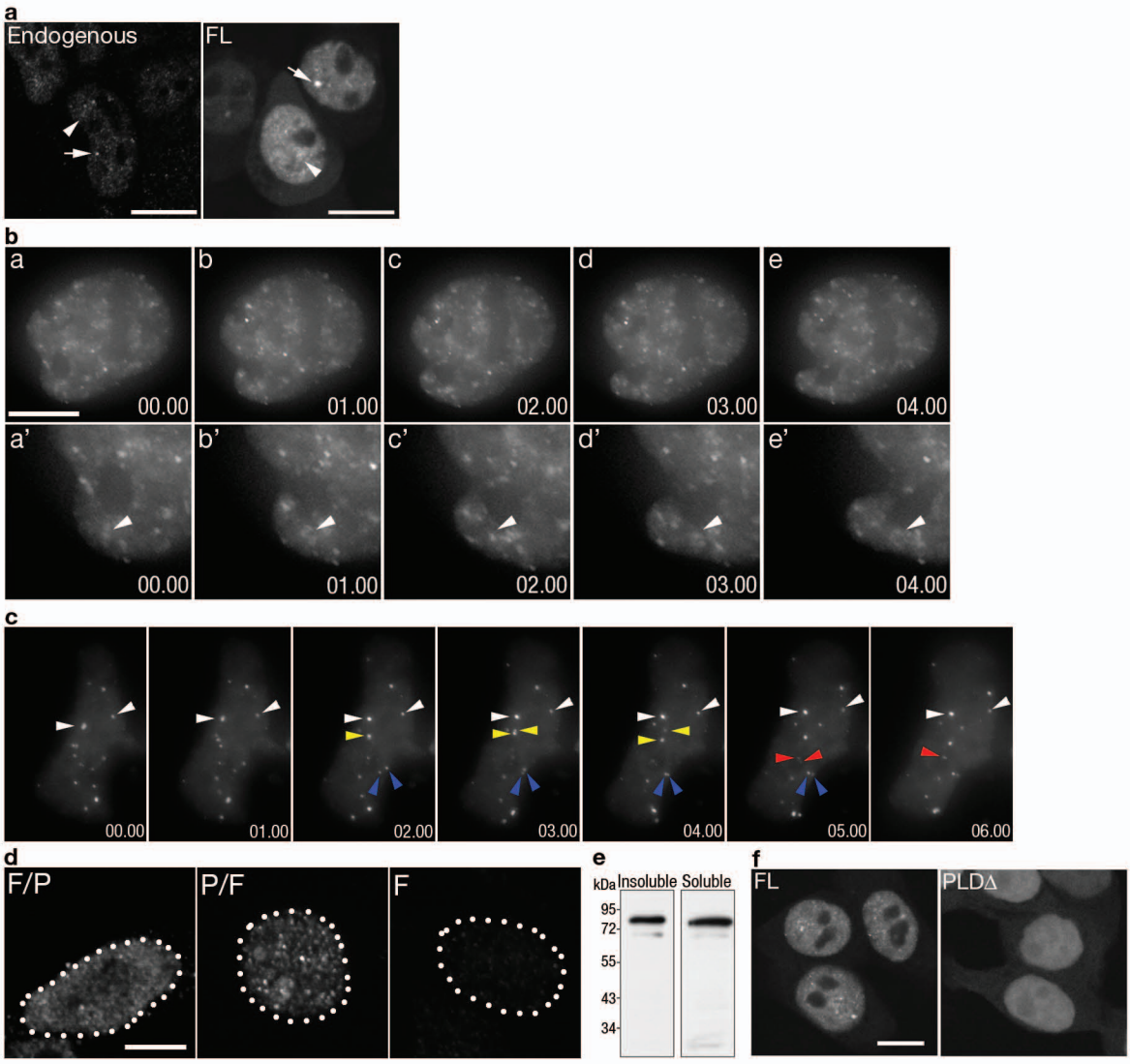
a
Endogenous
FL
b
a
b
c
d
e
00.00
01.00
02.00
03.00
04.00
a'
b'
c'
d'
e'
00.00
01.00
02.00
03.00
04.00
c
00.00
01.00
02.00
03.00
04.00
05.00
06.00
d
F/P
P/F
F
e
kDa
Insoluble
Soluble
95
72
55
43
34
f
FL
PLDΔ

Figure 2

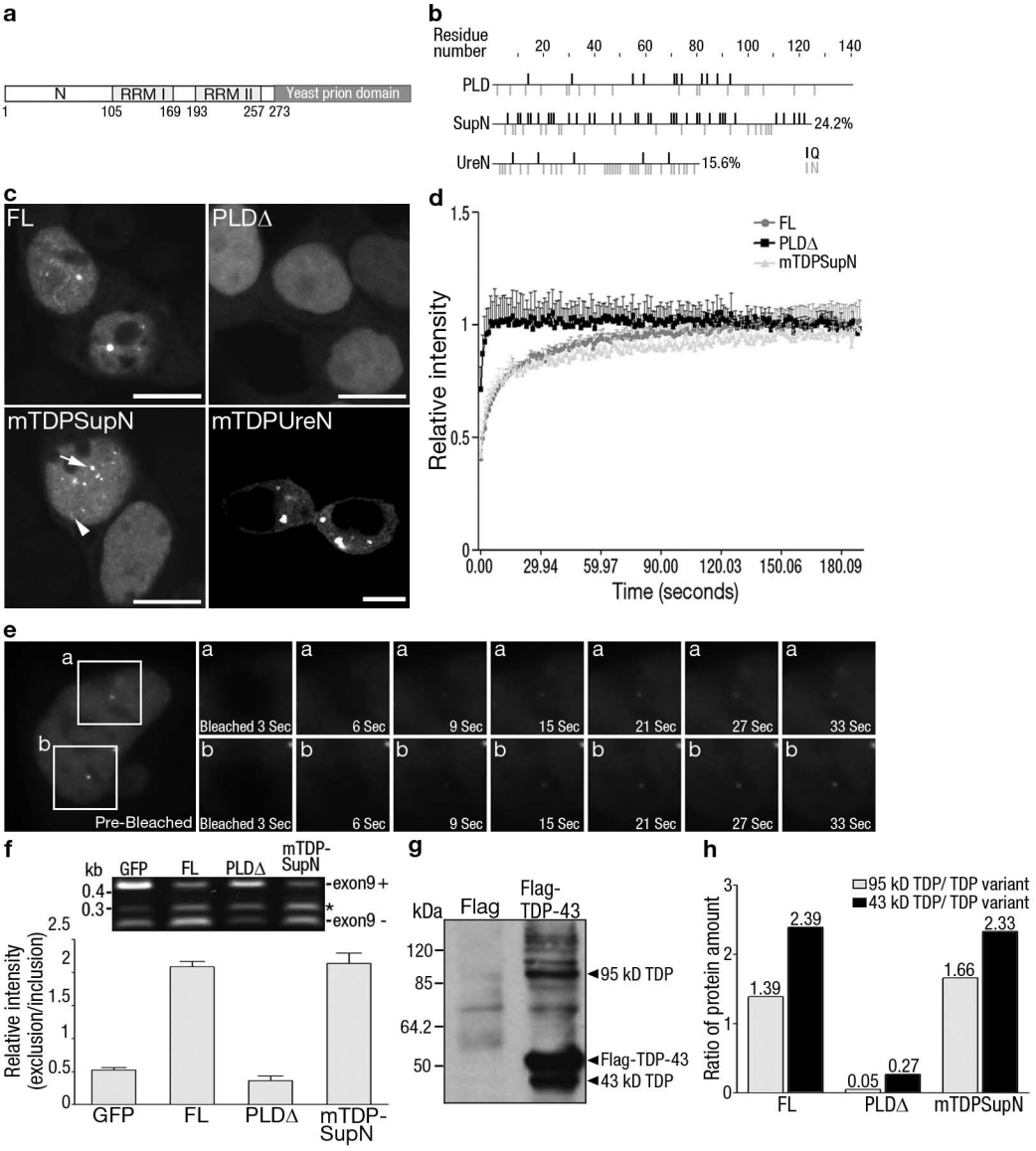
a
N
RRM I
RRM II
Yeast prion domain
1
105
169 193
257 273
b
Residue number
20
40
60
80
100
120
140
PLD
SupN
24.2%
UreN
15.6%
IQ
c
FL
PLDΔ
mTDPSupN
mTDPUreN
d
FL
PLDΔ
mTDPSupN
Relative intensity
1.5
1
0.5
0
0.00
29.94
59.97
90.00
120.03
150.06
180.09
Time (seconds)
e
a
b
Pre-Bleached
Bleached 3 Sec
6 Sec
9 Sec
15 Sec
21 Sec
27 Sec
33 Sec
f
kb
GFP
FL
PLDΔ
mTDP-SupN
0.4
0.3
-exon9+
*
-exon9 -
Relative intensity (exclusion/inclusion)
2.5
2
1.5
1
0.5
0
GFP
FL
PLDΔ
mTDP-SupN
g
kDa
Flag
Flag-TDP-43
120
85
64.2
50
95 kD TDP
Flag-TDP-43
43 kD TDP
h
95 kD TDP/ TDP variant
43 kD TDP/ TDP variant
Ratio of protein amount
3
2
1
0
1.39
2.39
0.05
0.27
1.66
2.33
FL
PLDΔ
mTDPSupN

Figure 3

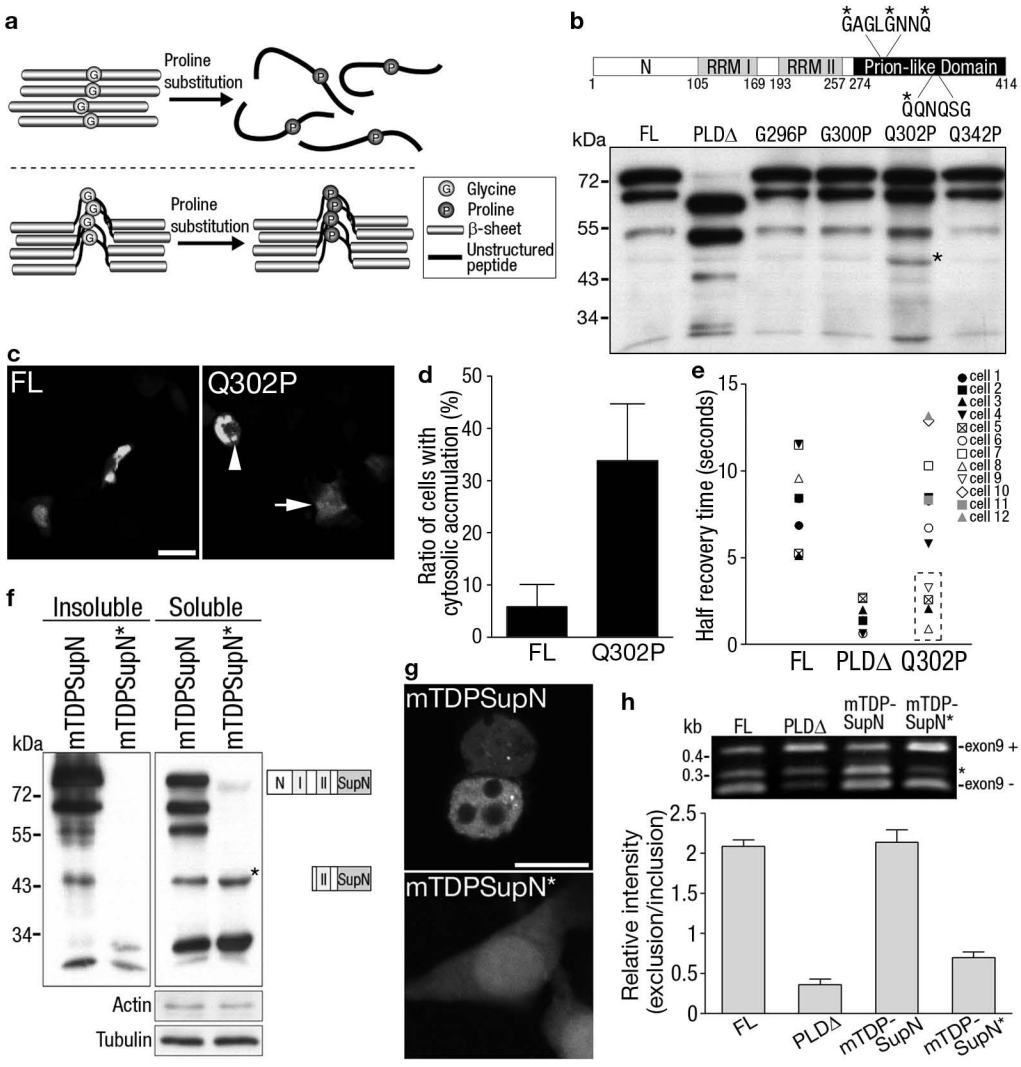
a
Proline substitution
Proline substitution
Glycine
Proline
β-sheet
Unstructured peptide
b
GAGLGNNQ
N
RRM I
RRM II
Prion-like Domain
1
105
169 193
257 274
414
QQNQSG
kDa
FL
PLDΔ
G296P
G300P
Q302P
Q342P
72
55
43
34
c
FL
Q302P
d
Ratio of cells with cytosolic accmulation (%)
50
40
30
20
10
0
FL
Q302P
e
Half recovery time (seconds)
15
10
5
0
FL
PLDΔ
Q302P
cell 1
cell 2
cell 3
cell 4
cell 5
cell 6
cell 7
cell 8
cell 9
cell 10
cell 11
cell 12
f
Insoluble
Soluble
mTDPSupN
mTDPSupN*
mTDPSupN
mTDPSupN*
kDa
72
55
43
34
N
I
II
SupN
II
SupN
Actin
Tubulin
g
mTDPSupN
mTDPSupN*
h
kb
FL
PLDΔ
mTDP-SupN
mTDP-SupN*
0.4
0.3
exon9 +
exon9 -
Relative intensity (exclusion/inclusion)
2.5
2
1.5
1
0.5
0
FL
PLDΔ
mTDP-SupN
mTDP-SupN*

Figure 4

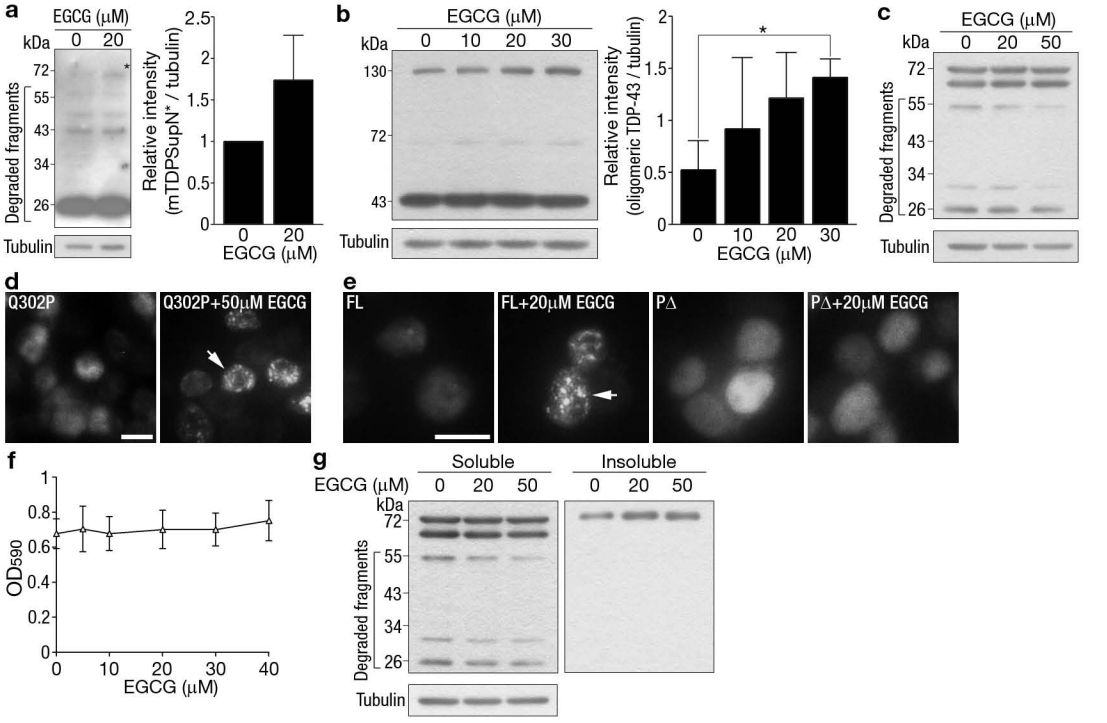
a
EGCG (μM)
kDa
0
20
72
55
43
34
26
Degraded fragments
Tubulin
Relative intensity (mTDPSupN* / tubulin)
2.5
2
1.5
1
0.5
0
0
20
EGCG (μM)
b
EGCG (μM)
kDa
0
10
20
30
130
72
43
Tubulin
Relative intensity (oligomeric TDP-43 / tubulin)
2
1.5
1
0.5
0
*
0
10
20
30
EGCG (μM)
c
EGCG (μM)
kDa
0
20
50
72
55
43
34
26
Degraded fragments
Tubulin
d
Q302P
Q302P+50μM EGCG
e
FL
FL+20μM EGCG
PΔ
PΔ+20μM EGCG
f
OD590
1
0.8
0.6
0.4
0.2
0
0
10
20
30
40
EGCG (μM)
g
Soluble
Insoluble
EGCG (μM)
0
20
50
0
20
50
kDa
72
55
43
34
26
Degraded fragments
Tubulin

Figure 5

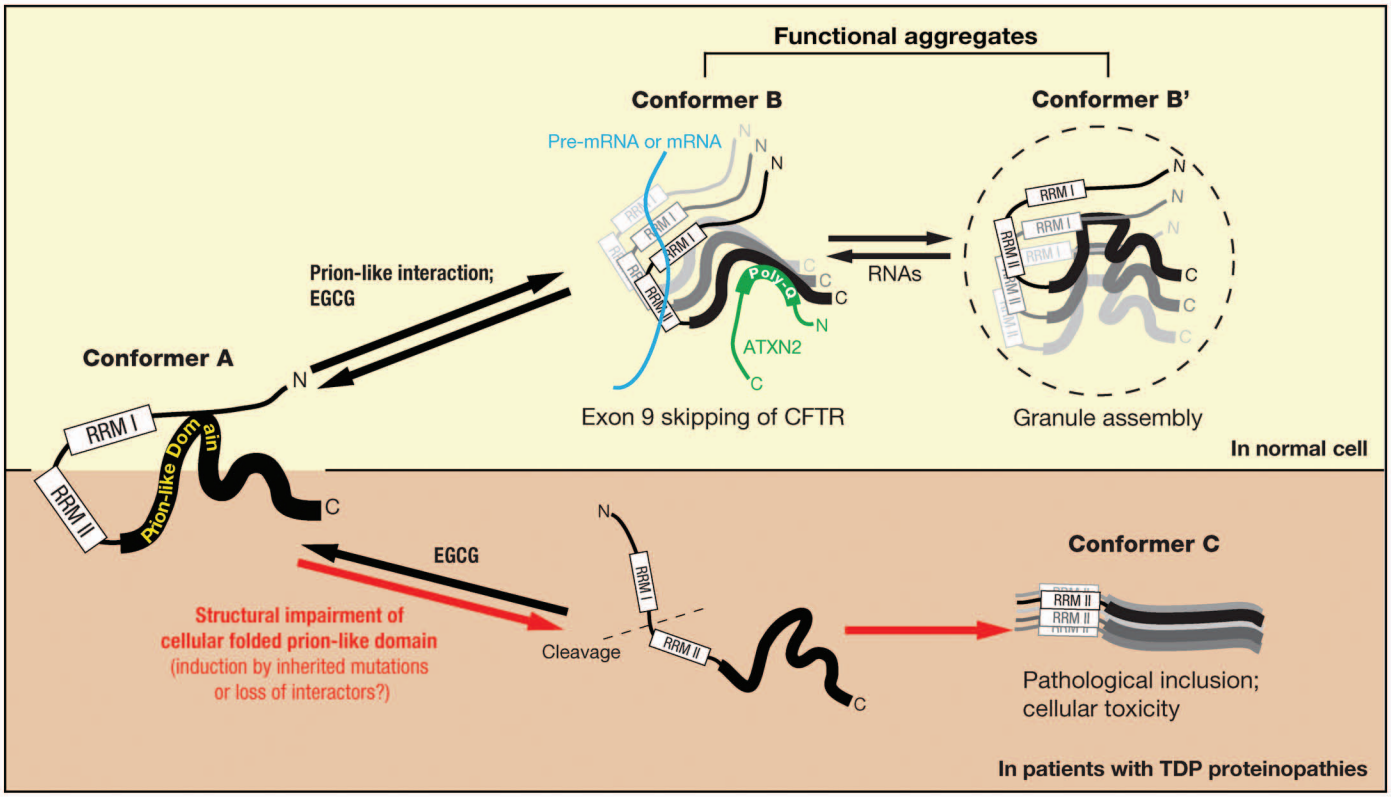
Functional aggregates
Conformer B
Conformer B'
Pre-mRNA or mRNA
RRM I
RRM II
Poly-Q
ATXN2
RNAs
Prion-like interaction;
EGCG
Conformer A
Prion-like Domain
Exon 9 skipping of CFTR
Granule assembly
In normal cell
EGCG
Structural impairment of
cellular folded prion-like domain
(induction by inherited mutations
or loss of interactors?)
Cleavage
Conformer C
Pathological inclusion;
cellular toxicity
In patients with TDP proteinopathies

Table 1. Properties of Cellular Folding and Misfolding of Q/N-rich Domain

		Cellular properties	Misfolded properties
Prionogenicity	Non-chromosomal genetic element	ND	y
	β-sheet rich structure	y[30]	y; Some form self-propagating amyloids (prions; ref. 29)
	Self-propagation	ND	y[21,22]
Prone-to-aggregate via an intrinsic element		y	y[21,22]
Cross interaction with other aggregation-prone proteins		y	y[16,24,28]
Structure variants		ND	y[26,33]
Solubility		Insoluble	Insoluble[21,22]
Toxicity		n	y (in mammals; ref. 20)
Signaling inducible oligomerization		y[31]	n
Dynamics		y	n
Biological roles		Alternative splicing; Protein stability; Granular assembly[25,27]; Nuclear-cytoplasmic exchange[30]; Long term facilitation in Aplysia[31].	Pathogenic factor[20]; Although yeast prions do not affect cell viability, they are proposed to be disadvantages to the hosts[23].

ND: not detected.